Formation of sprays from conical liquid sheets

By Bill Peck AND N. N. Mansour

1. Motivation and objectives .

Our objective is to predict droplet size distributions created by fuel injector nozzles in jet turbines. These results will be used to determine the initial conditions for numerical simulations of the combustion process in gas turbine combustors. To predict the droplet size distribution, we are currently constructing a numerical model to understand the instability and breakup of thin conical liquid sheets. This geometry serves as a simplified model of the liquid jet emerging from a real nozzle.

The physics of this process is difficult to study experimentally as the time and length scales are very short. From existing photographic data, it does seem clear that three-dimensional effects such as the formation of streamwise ligaments and the pulling back of the sheet at its edges under the action of surface tension are important.

A large body of analytic work on the linear stability of plane sheets exists (Squire, 1953; Hagerty and Shea, 1955). These papers found the sinuous mode (antisymmetric mode) to be most unstable but concluded that disintegration of the sheet could not be predicted. This follows since the linear analysis does not predict thinning of the sheet. The nonlinear planar problem has been studied using asymptotic methods (Clark and Dombrowski, 1972), and more recently a reduced dimension technique has been used by, Mehring and Sirigano (1999). These analyses predict a thinning of the sheet that may lead to the sheet breakup and disintegration. Analysis of more general geometries has been limited although Mehring and Sirigano (2000) have recently started work on analysis of a conical sheet with their reduced-dimension technique. In the future, analytic work with directed fluid sheets using techniques similar to those used by Bogy (1979) for liquid jets may be of some use.

Modeling the expected behavior of the conical sheet will require a fully three-dimensional code. Numerical simulations of the breakup of three-dimensional liquid sheets have been limited. These calculations are difficult due to problems with accurately tracking fluid interfaces and gross topological changes. Several techniques have evolved to address the difficulties associated with having a surfaces of discontinuity embedded in a three-dimensional domain. Such methods include: Level Set methods, Sethian (1999), Volume of Fluid methods Zaleski (1999) and Front Tracking schemes, Unverdi & Tryggvason (1992). Finite element techniques have also been used for interface problems and offer attractive accuracy but are computationally very expensive, and, so far, topological changes have not been implemented.

For our work we have chosen to develop a front tracking code based on the method used by Tryggvason's group. This method tracks material particles on the interface from which material property fields such as density and viscosity are constructed
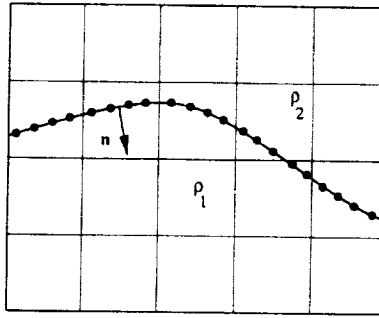
Fig. 1. A fixed two-dimensional grid with an embedded surface constructed from material points separating two regions of fluid with disparate material properties.

at each time step. A field of surface forces is also calculated based on the front's location and geometry.

By keeping track of material points on the interface, this scheme also offers a means to control topological changes and introduce physics that control such occurrences. These changes are typically due to processes at the molecular level. Adding this capability to front tracking schemes is currently an active area of research.

We are also interested in developing this code to understand the instability of a thin liquid film lying between a solid surface and an incompressible gas flowing over it. This has applications in atomizers and hybrid rocket engines. For this situation we intend to use a planar two-dimensional simulation to understand the instability and predict droplet formation. The results given below are from the interface tracking scheme to be used with this code.

2. Accomplishments

In this section we describe the two-dimensional code we are writing using the interface tracking technique developed by Tryggvason's group (Uneverdi and Tryggvason, 1992). Although this section describes a two-dimensional interface tracking method, it illustrates the basic methodology used for the three-dimensional case.

A unique feature of interface tracking schemes is the ability to follow the motion of material particles embedded in the interface as shown in Fig. 1. This introduces several extra complexities into the code needed to keep track of the location and properties of the surface. However, language features such as pointers and structures found in modern programming languages allow us to easily construct data structures that greatly simplify this task.

2.1 Front tracking algorithm

The front tracking scheme uses a fixed grid through which a material interface is convected. The material interface is represented by a discrete series of points representing the location of the front. Material properties are allowed to jump across the interface. The material particles are convected at each time step, and new material property fields and surface force fields are calculated based on the position of points on the front.

Equations of motion

A form of the Navier-Stokes equations that includes effects of stresses intrinsic to a surface of discontinuity embedded in the domain is written as

$$\frac{\partial \rho \mathbf{u}}{\partial t} + \text{div}(\rho \mathbf{u} \otimes \mathbf{u}) = -\text{grad}p + \rho \mathbf{f} + \text{div}[\mu(\text{grad}\mathbf{u} + \text{grad}\mathbf{u}^{\mathrm{T}})]$$
$$+ 2 \int H\gamma \mathbf{n}\delta^{\beta}(\mathbf{r} - \mathbf{r}_s)ds. \tag{1}$$

Here ρ represents density, μ viscosity, p pressure, $\mathbf{u}$ fluid velocity, and $\mathbf{f}$ are body forces. γ is surface tension, H is mean curvature, and $\mathbf{r}$ is the position vector of an arbitrary point in the domain while $\mathbf{r}_s$ is a point on the surface. The vector $\mathbf{n}$ is the unit normal to the surface of the interface, and δ^{β} is the multi-dimensional delta function. This equation is valid over the entire domain (Unverdi & Tryggvason 1992).

Material properties of material particles are assumed to remain constant in time so that $\dot{\rho} = 0$ and $\dot{\mu} = 0$. Now the mass conservation equation

$$\frac{\partial \rho}{\partial t} + \text{div}(\rho \mathbf{u}) = 0,$$

simply becomes

$$\text{div}(\mathbf{u}) = 0. \tag{2}$$

Equation 1 is discretized onto the fixed grid using standard schemes. An important difference with standard incompressible DNS codes is that the effects of surface forces are included on the fixed grid and material properties are spatially variable although the flow is incompressible. The density variation leads to a non-separable PDE for the pressure equation that does not allow the use of fast Poisson-type solvers. As a result, the pressure equation is usually solved using multi-grid solvers such as MUDPAK, which substantially increases computational time.

Description of the front

The front is represented by a series of FORTRAN 90, TYPE structures connected by pointers to form a doubly-linked list. A linked list is a natural metaphor for the material front; each node of the structure contains information pertinent to that point on the interface. Variables such as position, arc-length, and varying intrinsic surface properties can easily be stored in each node structure.

Each node of the linked list represents an endpoint of a surface element. This data structure allows us to easily insert or remove surface elements by inserting nodes as the front is stretched or compressed. The insertion-extraction scheme is adjusted to give about four elements per grid-cell. The position of new nodes is determined by simple polynomial interpolation.

Construction of material property fields

Fluid properties in the bulk regions are constructed at each time step based on the updated location of the interface. This includes constructing a field of surface forces that are transferred from the front to the fixed grid.

The scheme for constructing the density field follows. First, we note that the density gradient can be expressed as

$$\mathrm{grad}\rho = \int \Delta\rho\mathbf{n}\delta(\mathbf{r} - \mathbf{r}_s)ds$$

where $\Delta\rho$ is the jump in density across the interface. The subscript s denotes values on the surface. $\mathbf{n}$ is the unit normal as used in Eq. 1 and is oriented such that

$$\mathbf{n} = \frac{\mathrm{grad}\rho}{\|\mathrm{grad}\rho\|}.$$

A value for $\mathrm{grad}\rho$ on the fixed grid is calculated by using a suitable weighting function, w_{ijk}, to transfer information from the front to the fixed grid. w_{ijk} is the product of n one-dimensional functions:

$$w_{ijk}(\mathbf{r}_s) = d(x_s - x)d(y_s - y)d(z_s - z). \tag{3}$$

Here x, y, z are the coordinates of the fixed grid and x_s, y_s, z_s are coordinates of a point on the surface. $\mathbf{r}_s$ is the position of a point on the surface so that $w_{ijk}(\mathbf{r}_s)$ is the weighting on a fixed grid point due to a surface element at $\mathbf{r}_s$. In our work so far we have used the function first used by Peskin (1977) and now commonly used:

$$d(r) = \begin{cases} \frac{(1+cos(\pi r/2h)}{2h}, & \|r\| < 2h, \\ 0, & \|r\| \geq 2h, \end{cases} \tag{4}$$

where $r = \|\mathbf{r} - \mathbf{r}_s\|$.

After visiting each node on the interface, we are left with a smoothed approximation to the derivative across the interface. Examples of the smoothed density gradient are shown in Fig. 2 and Fig. 3. The density ratio is 10:1 with the fluid surrounding the drop assumed to have a unit density.

Taking the numerical divergence of the density gradient yields a Poisson equation for the density field:

$$\mathrm{div}(\mathrm{grad}\rho) = \mathrm{div}_h\mathrm{grad}\rho_{ij} \tag{5}$$

The term on the right denotes the numerical divergence of the grid density gradient field. This equation is readily solved for ρ with appropriate boundary conditions using fast-Poisson solvers such as the routines found in FISHPACK. The smoothed reconstructed field is shown in Fig. 4 . The viscosity field is reconstructed in the same way.

Surface forces

Numerical simulations of interfacial problems with surface tension introduce several difficulties. In the scheme discussed here surface forces are transferred to the front in a similar manner as discussed above for the density field.
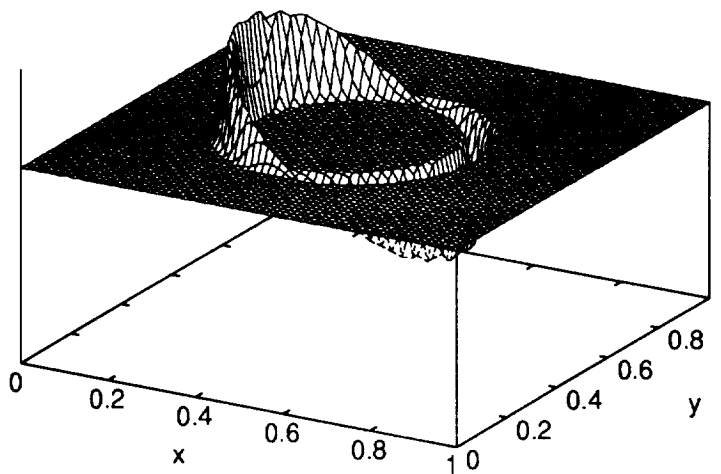
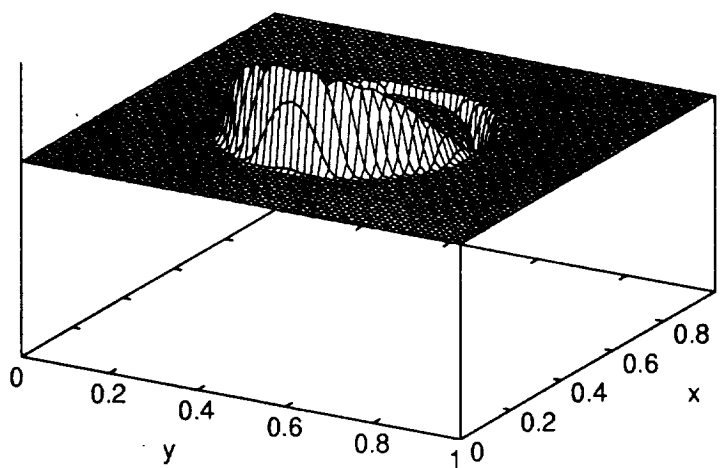Fig. 2. x-directed density gradient field on a 64 × 64 grid.

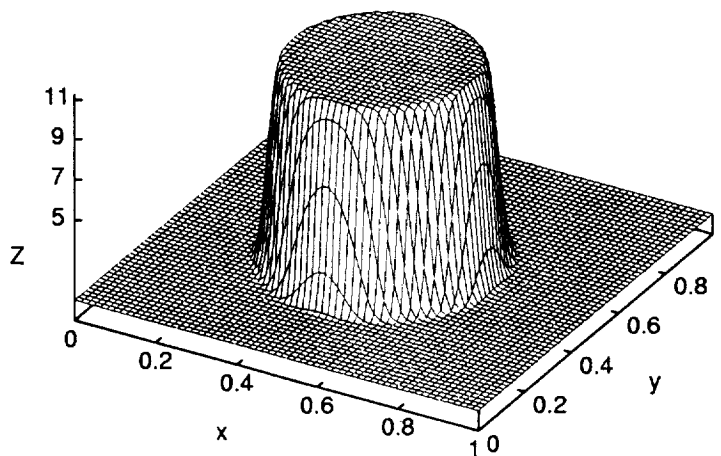Fig. 3. y-directed density gradient field on a 64 × 64 grid.

Fig. 4. Reconstructed density field on a 64 × 64 grid. The base density is 1.0 and $\Delta\rho = 10.0$.
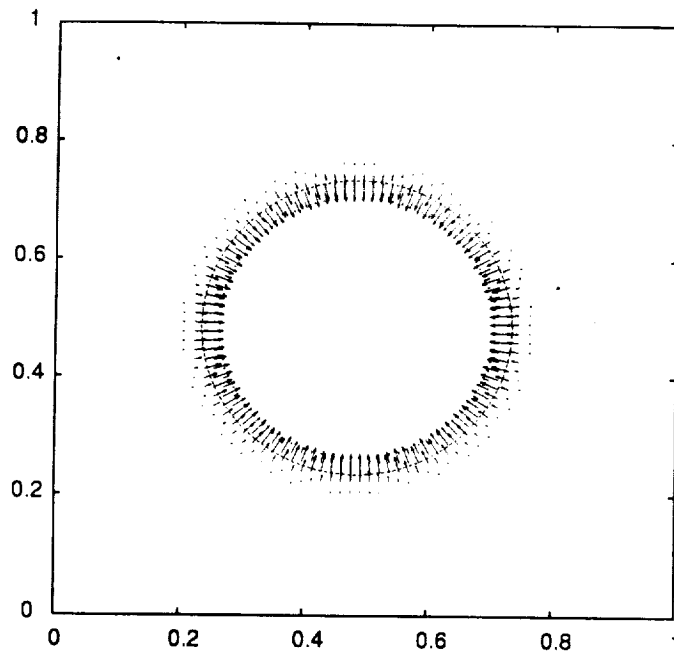
Fig. 5. Surface forces transferred to the fixed 64 × 64 grid from an initially circular drop.
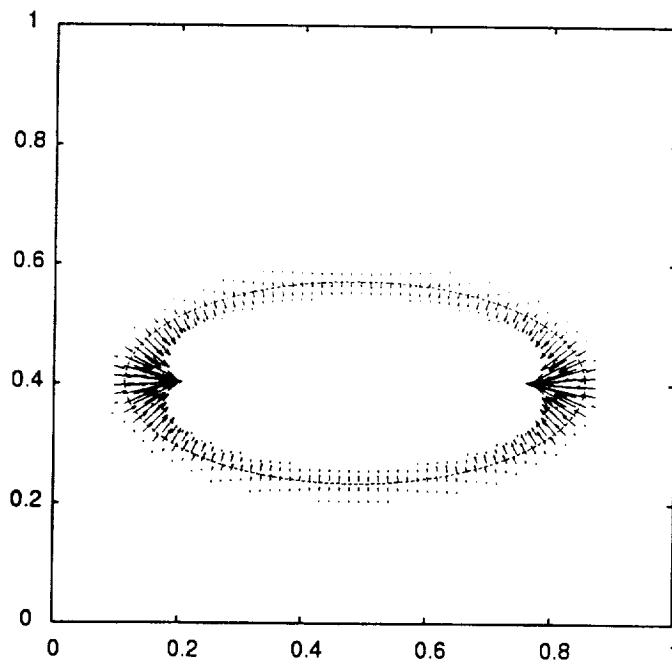

Fig. 6. Surface forces transferred to a fixed grid after the drop has been deformed in a stagnation point flow. Several surface points have been added in areas where the surface has been stretched and several deleted in the regions of higher curvature where the surface has been compressed.

For two-dimensional in the plane, mean curvature simply becomes the curvature of the plane curve marking the interface. The force transferred to the bulk fluid due to a surface element of length ds is then given by

$$\int_{s_1}^{s_2} \kappa \gamma \hat{n} ds = \gamma \int_{s_1}^{s_2} \frac{\partial t(s)}{\partial s} ds = \gamma (t_2 - t_1). \qquad (6)$$

Here, κ is the curvature and $\hat{n}$ is the normal to the plane curve in the sense of the Frenet formulae. That is, it points toward the center of curvature of the plane curve and not necessarily in the direction of n, which acquires its direction from a gradient in the density field.

As with the density field, we visit each surface element in the linked list that represents the front. At each node, the unit tangents t_1 and t_2 at each end of the line element are calculated. In two dimensions, the integrated effect of the surface tension forces over the element length is simply the vector difference in the unit tangent vectors of node points at the end of the surface element as shown in Eq. 6.

After visiting all the points on the front we have a field of surface forces transferred to the fixed grid as shown in Fig. 5 and Fig. 6. Figure 5 illustrates the surface force field created by an initially circular "drop". Figure 6 shows the surface force field after the drop has been strained into an ellipse. The greater values of surface forces transferred to the fixed grid are apparent in the deformed case due to the higher curvatures at the right and left ends of the drop.

3. Future plans

In the next year we intend to complete a two-dimensional planar and axisymmetric front-tracking code. This code will be used to study the instability and drop formation of a thin sheet lying on a solid surface. This work will expand on the present effort, leading to more sophisticated models that incorporate phase change as well as topological changes.

A substantial challenge for the forthcoming year will be the implementation of a fully three-dimensional code, which is ultimately what we require to study the conical jet. As with the two-dimensional code, the greatest obstacle to overcome is accurate representation of the front and construction of fluid property fields. In three-dimensions the primary difference is that the front is represented as a collection of two-dimensional surface elements. The size and distribution of these elements must be adjusted with time as surface elements become too small or large.

A major difficulty in three-dimensional codes is the accurate calculation of surface curvature. At present most front-tracking schemes use fitted ellipsoids to estimate the local curvature. We hope to construct a scheme that uses the coordinates of the centers of the surface elements.

Also, alternative techniques have been developed by Popinet and Zaleski (1999) to transfer surface forces onto the fixed grid in two-dimensions. These authors have reported that this technique reduces spurious currents found in other schemes due to smoothing surface stresses onto the fixed grid. Their techniques should, in principle, be adaptable to three-dimensional cases.

In the front tracking scheme, the underlying differencing grid is a uniform stationary mesh. In general, to obtain a manageable computation, the grid is a compromise between resolving the small length scales at the interface and computational power. Adapting the grid to a finer resolution near the interface where relevant length scales are small compared to the bulk flow is one solution. This technique has been implemented in two dimensions by Agresar *et al.* (1998) to study biological cell mechanics. Its implementation in three-dimensions will be investigated.

Acknowledgments

REFERENCES

AGRESAR, G. & J. J. LINDERMANN , & TRYGGVASON, G., & POWELL, K. G. 1998 An adaptive, cartesian, front-tracking method for the motion, deformation and adhesion of circulating cells. *J. Comp. Phys.* **143**, 346-380.

BOGY, D. B. 1979 Drop formation in a circular liquid jet. *Ann. Rev. Fluid Mech.* **1979.**

CLARK, C. J. & DOMBROWSKI, N. 1972 Aerodynamic instability and disintegration of inviscid liquid sheets. *Proc. R. Soc. London.* **A329**, 467-478.

HAGERTY, W. W. & SHEA, J. F. 1955 A study of the stability of plane fluid sheets. *J. Appl. Mech.* **22**, 509-514.

MEHRING, C. & SIRIGANO, W. A. 1999 Nonlinear capillary wave distortion and disintegration of thin planar liquid sheets. *J. Fluid Mech.* **388**, 69-113.

MEHRING, C. & SIRIGANO, W. A. 2000 Nonlinear capillary wave distortion and disintegration of thin planar liquid sheets. *To be presented at the 2000 AIAA meeting.* **388**, 69-113.

PESKIN, C. S. 1977 Numerical analysis of blood flow in the heart. *J. Comp. Phys.* **25**, 220-252.

POPINET, S. & ZALESKI, S. 1999 A front tracking algorithm for accurate representation of surface tension. *Int. J. Num. Meth. Fluids.* **30**, 775-793.

SCARDOVELLI, R & ZALESKI, S. 1999 Direct numerical simulation of free-surface and interfacial flow. *Ann. Rev. Fluid Mech.* **31**, 567-603.

SETHIAN, J. A. 1999 *Level Set Methods and Fast Marching Methods,* Cambridge University Press.

SQUIRE, H. B. 1953 Investigation of the instability of a moving liquid film. *Br. J. appl Phys.* **4**, 167-169.

UNVERDI, S. O. & TRYGGVASON, G. 1992 A front-tracking method for viscous, incompressible multi-fluid flows. *J. Comp. Phys.* **100**, 25-37.